natural science

Genetic Structure and Diversity of the Medano-Zapata Bison Herd using Microsatellite Data

Torrey Davis

The following is an excerpt from a longer piece. For full text, please visit www.honorsjournal.com.

ABSTRACT

IN THE LATE 1800s, the American plains bison (*Bison bison*) suffered from a severe reduction in population size, known as a bottleneck event. Their numbers, once in the millions, were reduced to less than a thousand individuals, but populations were able to recover owing to the diligence of several private ranchers and other private and governmental groups. While bison populations have improved today, their genetic diversity has been impacted by the bottleneck event, habitat fragmentation, and hybridization with domestic cattle (*Bos taurus*). With advances in genetic technology, it is now possible to gather genetic information of a species to aid in their conservation. Here, using genetics software, I analyzed nuclear genetic data previously used to detect cattle genes in the Medano-Zapata bison herd located in Colorado, USA. I was able to determine (1) the number of genetic clusters and (2) calculate different indices of genetic variation to estimate population viability. I hypothesized that more than one cluster would occur within the population due to its large size. My results rejected this hypothesis, with the strongest likelihood supporting a single cluster. This information is important for understanding the genetic diversity of the herd. It is also important for understanding the impacts of cattle genes on bison populations and what they mean for the species' future conservation.

INTRODUCTION

The North American plains bison (*Bison bison*) is an iconic species of the American west that historically ranged from Canada to Mexico, and from the west to east coasts of North America (List et al. 2007; Sanderson et al. 2008). In the late 1800s, bison suffered from a significant population bottleneck, or severe reduction in their population. Once numbering in the millions, bison populations were reduced to less than a thousand individuals (Hedrick 2009) through overexploitation, habitat loss, and disease (Isenberg 2000). The species was saved from near extinction in the early 1900s through the diligence of five private ranching herds, a herd at the New York Zoological Park (Hedrick 2009), and a small, isolated herd in Yellowstone National Park (Meagher 1973). During this time, some of the private ranchers experimented with crossing bison and domestic cattle (*Bos taurus*) to promote disease resistance,

increase meat quality and quantity, and increase feeding efficiency and hardiness in their cattle stock (Boyd 1914; Goodnight 1914). Female cows were often bred with male bison, and the hybrid offspring were repeatedly backcrossed with male bison, leading to cattle gene introgression in the bison herds (Hedrick 2009). Hybridization between two species may lead to extinction of one of the species (Allendorf et al. 2001), and hybridization with a species that has been selected for domestic traits (such as cattle) may impact local adaptation of the threatened or endangered species (Randi 2008).

[…]

Approaches to quantify genetic characteristics of bison have been developed by researchers, including looking at multiple microsatellite loci in the nuclear genome (Halbert et al. 2005). Microsatellites, also known as short tandem repeats (STRs), are short, repetitive DNA sequences that occur throughout the genomes of many eukaryotes (Bhargava and Fuentes 2010). They are commonly used in population genetics analyses because they are thought to evolve neutrally (i.e. they are not influenced by natural selection) and are highly polymorphic, meaning they can have multiple variations, or alleles, at each locus (Putman and Carbone 2014).

The Medano-Zapata bison herd is a population of about 1,700 animals that is managed by The Na-

The Medano-Zapata bison herd is…managed by The Nature Conservancy in Colorado, USA. To better assess population viability for genetic management of this larger sample of the herd, here I analyzed the larger dataset to test for the presence of genetic substructure and genetic diversity ౷

ture Conservancy in Colorado, USA. It is routinely rounded up and hair and blood samples are collected. A recent project report by Halbert and Derr (2010) analyzed the genetic diversity from a subpopulation of the herd using 185 individuals and 11 polymorphic microsatellite markers. The report determined that the herd had high levels of genetic diversity (based on heterozygosity and number of alleles per locus) and was derived from at least three different source herds.

A separate study of the herd sampled 1,700 of the individuals and analyzed different 14 microsatellite markers to detect levels of cattle genetic introgression (12.59%) in the nuclear genome (Hamilton et al. 2009). This study did not, however, look at levels of genetic diversity (heterozygosity and number of alleles) using the 14 markers or assess whether any genetic structure in the entire herd existed. To better assess population viability for genetic management of this larger sample of the herd, here I analyzed the larger dataset to test for the presence of genetic substructure and genetic diversity. I hypothesized that multiple clusters would be found owing to the population being large and having a higher likelihood of different genetic groups forming. Additionally, I used the expanded samples size to obtain a more accurate estimate of the levels of genetic diversity present.

Data Collection

The microsatellite genetic data for the Medano-Zapata Ranch herd had previously been collected and archived at Texas A&M University. Previously established protocols (Halbert et al. 2005) were used to assess levels of cattle gene introgression at 14 diagnostic and polymorphic (containing more than one allele) microsatellite markers. The markers analyzed were: AGLA17, AGLA293, BM1314, BM4307, BM4513, BM7145, BMS2270, BMS4040, CSSM36, CSSM42, RM185, RM500, SPS113, and TGLA227. The markers spanned 10 chromosomes (of 30 total chromosomes in bison) and were used to either diagnose or confirm whether cattle gene introgression had occurred (Halbert et al. 2005).

Data Analysis

To analyze the structure of the population, I used STRUCTURE v. 2.3.4 (Pritchard et al. 2000) with the 14 microsatellite loci for all 1,700 individuals. I used the admixture model and ran seven repetitions for each K value (1-4), with K being the number of assumed genetic clusters and calculated the mean of logarithmic probability (Cao et al. 2017). I used a burn-in period of 500,000 steps and Monte Carlo Markov Chain (MCMC) rep length of 500,000 steps and chose the K genetic cluster values based on methods published in the literature (Pinzone and Dyer 2013).

The two indices of genetic diversity that I used were (1) expected heterozygosity (H_E) and (2) number of alleles and their associated frequencies. Expected heterozygosity is an indicator of genetic variation and provides information on the frequency of heterozygotes (markers containing different alleles, rather than the same alleles). For calculating expected heterozygosity in this study, I used the formula from Nei and Roychoudhury (1974) and used the allele frequencies calculated from my STRUCTURE analysis. I also summarized allelic data from the STRUCTURE analysis and summarized the number of alleles at each locus (including the cattle alleles) and their frequencies of occurrence within the population.

RESULTS

Genetic Clustering

From the STRUCTURE analysis, the most likely number of genetic clusters was K = 1 based on the highest average natural logarithm (Ln) of the likelihood across runs (average Ln =   -14547.2). Table 1 summariz-

K	Mean Estimated Ln Probability	Standard Error of Mean Estimated Probability
1	**-14547.2**	7.43E-13
2	-15003.2	13.09
3	-16017.1	99.84
4	-17142.6	137.86

Table 1. Results from the STRUCTURE analysis of the 14 microsatellite loci and associated standard error values. The value in bold indicates the highest support (K = 1) of the K clusters based on likelihood alone.

es the results from the analysis, and Supplementary Figure S1 plots the K values and shows the most probable likelihood value.

Indices of Genetic Diversity

The expected heterozygosity (H_E) is a measure of genetic variation based on the frequencies of each allele at each locus. The average H_E values for all 14 loci was close to 0 (H_E = 0.1860), indicating the diversity of alleles was low. Table 2 gives the H_E values for each locus.

The number of alleles at each locus ranged from 1 to 4. The total number of alleles identified was 36, and the mean number of alleles per locus was 2.57, which gives the expected number of alleles at any of the 14 given loci. Of the 14 markers used, 13 were polymorphic and RM500 was monomorphic with only one allele. The percentage of cattle alleles to the total number of alleles identified was 25%. From the analysis, I was able to determine the allele frequencies of both the bison and cattle alleles. Allelic frequencies give the prevalence of each allele within the population. The frequency of cattle allele occurrence at each locus ranged from 0.1% to 2.2% and the standard error was 0.069 (see Supplementary Table S1). Table 2 provides a summary of the allelic information at each of the 14 loci, including which chromosomes they are located on and which alleles are considered indicative of domestic cattle gene introgression. (Table pictured below)

DISCUSSION

Genetic Clustering

The results of this study most strongly supported genetic clustering around a single cluster and reject-

Locus	Number of alleles	Alleles (bp)	H_E	Chromosome (n = 30)
AGLA17	2	215, 218	0.004	1
AGLA293	4	218, 215, 220, 228*	0.080	5
BM1314	2	137, 157*	0.033	26
BM4307	4	185, 187, 197*, 189*	0.340	1
BM4513	2	132, 134	0.220	14
BM7145	3	108, 110, 116*	0.307	1
BMS2270	4	66, 68, 70, 98**	0.553	24
BMS4040	2	75, 95**	0.002	1
CSSM36	2	132, 158	0.000	27
CSSM42	3	167, 171, 169	0.570	2
RM185	2	92, 100*	0.004	23
RM500	1	123	0.000	5
SPS113	3	130, 132, 128	0.476	10
TGLA227	2	73, 94**	0.012	18

Table 2. A summary of information on the 14 polymorphic microsatellite loci that were used for the analysis. * Is a confirmed domestic cattle allele and ** is a suspected diagnostic cattle allele (see Halbert et al. 2005). Chromosome location and domestic cattle allele information are adapted from Halbert et al. (2005).

ed my hypothesis that there would be multiple clusters. This indicates that the individuals are part of one interbreeding, or admixing, population and that genes are randomly distributed among individuals. Admixture occurs when individuals from two or more genetically differentiated populations interbreed and gene flow occurs (Rius and Darling 2014). In addition, the effects of the historic bottleneck are likely to have reduced the genetic variation within the loci. The difference in mean estimated natural log probabilities between $K = 1$ and $K = 2$, however, is closer than the other clusters, hinting that perhaps two clusters are forming in the population. Future studies could potentially investigate this effect using more genetic loci.

[…]

Indices of Genetic Diversity

The mean expected heterozygosity was relatively low for the markers used in this study and the total number of alleles at the 14 markers was also low. Heterozygosity is commonly used as a measure of genetic variation and the values are expressed as the frequency of heterozygotes (i.e. the alleles are different at each locus). It is likely that the low value in the Medano-Zapata bison population is a consequence of the historical bottleneck. Typically, after a bottleneck event, heterozygosity levels are expected to decline due to a random loss of alleles (Allendorf and Leary 1986; Nei et al. 1975). A population reduction can also result in inbreeding, or the mating between closely related individuals. Inbreeding increases the proportion of homozygotes (thereby reducing heterozygosity) and can also increase

the probability of deleterious alleles. Additionally, the sudden loss of genetic variation can potentially affect the population's effective population size and decrease its evolutionary potential by reducing variability that can be passed on to the next generation (Nei et al. 1975).

The frequencies of occurrence of the cattle alleles were low but did vary depending on the locus. AGLA293 contained a cattle allele that occurred the most frequently, while BMS4040 had an allele that occurred at a very low frequency. This variation in frequencies is likely due to chance genetic drift, which allows the alleles to persist at low levels (see Hedrick 2009). Whether these nuclear alleles have any effect on the phenotype, or physical expression of the genes, is unclear. In a study by Derr et al. (2012), the researchers found that high levels of mitochondrial cattle introgression resulted in smaller body sizes in bison. Whether the smaller body size had any effect on the fitness of the bison was less clear, but generally there is a positive relationship between body size and fitness (Robertson 1955). Future studies could address if there are any positive (advantageous) or negative (deleterious) phenotypic effects on nuclear cattle alleles in bison populations.

Conclusions

While the 14 loci used in this study are indicative of cattle gene introgression levels, when analyzed at the genetic structure level, they provide interesting clustering results and indicators of genetic diversity that are worth investigating and understanding further. To provide a better resolution of genetic diversity in future genetic analyses, it is worth looking at multiple microsatellite

42

loci distributed across the genome (Chambers and MacAvoy 2000).

The Medano-Zapata herd is a relatively large herd with more than 1,000 individuals that roam a large landscape. As such, it is one of the few large conservation herds that is managed as a semi-wild herd, and the protection and evaluation of its genetic features is worth continued investigation. This includes understanding and increasing the herd's effective population size by assessing differential breeding of males and females (i.e. is one male mating more often than other males and disproportionately contributing to the next generation?) and maintaining roughly equal sex ratios (Gates et al. 2010). In addition, it is important to continue protecting the bison's habitat and increase the connectivity between different populations. By intermixing bison populations, their genetic diversity can increase overall. Plains bison historically covered large territories, and they likely had high rates of gene flow when they were able to intermix (Berger and Cunningham 1994; Wilson and Strobeck 1999). Lastly, continued investigation of the levels of cattle gene introgression and how to effectively manage introgression levels is worth considering in future research and management.

Works Cited

Allendorf FW, Leary RF (1986) Heterozygosity and fitness in natural populations of animals. In: *Conservation Biology: the Science of Scarcity and Diversity*. Sinauer Associates, Incorporated, New York.

Allendorf FW, Leary RF, Spruell P, Wenburg JK (2001) The problems with hybrids: setting conservation guidelines. *Trends in Ecology and Evolution*, **16**, 613-622.

Berger J, Cunningham C (1994) Bison: mating and conservation in small populations. In: *Methods and Cases in Conservation Science.* Columbia University Press, New York.

Beebee T, Rowe G (2008) *An Introduction to Molecular Ecology*. Oxford University Press, Oxford.

Bhargava A, Fuentes FF (2010) Mutational dynamics of microsatellites. *Molecular Biotechnology*, **44**, 250–266.

Boyd, DP (2003) Conservation of North American bison: status and recommendations. MS Thesis, University of Calgary.

Boyd, MM (1914) Crossing bison and cattle. *Journal of Heredity*, **5**, 189–197.

Cao J, Li X, Du X, Zhao S (2017) Microsatellite based genetic diversity and population structure of nine indigenous Chinese domestic goats. *Small Ruminant Research*, **148**, 80–86.

Chambers GK, MacAvoy ES (2000) Microsatellites: consensus and controversy. *Comparative Biochemistry and Physiology Part B: Biochemistry and Molecular Biology*, **126(4)**, 455–476.

Coder GD (1975) The national movement to preserve the American

buffalo in the United States and Canada between 1880 and 1920. PhD Thesis, Ohio State University.

Dary DA (1989) *The Buffalo Book: the Full Saga of the American Animal*. Swallow Press, Chicago.

Derr JM, Hedrick PW, Halbert ND et al. (2012) Phenotypic effects of cattle mitochondrial DNA in American bison. *Society for Conservation Biology*, **26**(6), 1130-1136.

Freese CH, Aune KE, Boyd DP et al. (2007) Second chance for the plains bison. *Biological Conservation*, **136**, 175–184.

Gates CC, Freese CH, Gogan PJP, Kotzman M (2010) American bison: status survey and conservation guidelines. IUCN, Gland, Switzerland.

Goodnight C (1914) My experience with bison hybrids. *Journal of Heredity*, **5**, 197–199.

Halbert ND, Derr JN (2010) Bison Genetics of the Great Sand Dunes National Park. Final Project Report, Texas A&M University.

Halbert ND, Ward TJ, Schnabel RD et al. (2005) Conservation genomics: disequilibrium mapping of domestic cattle chromosomal segments in North American bison populations. *Molecular Ecology*, **14**, 2343– 2362.

Hamilton RG, Halbert ND, Derr JN (2009) Bison herd genetic architecture and management – working toward a species-wide conservation approach. Final Project Report, The Nature Conservancy.

Hedrick PW (2009) Conservation genetics and North American bison (*Bison bison*). *Journal of Heredity*, **100**, 411–420.

Isenberg AC (2000) *The Destruction of the Bison: an Environmental History, 1750-1920*. Cambridge University Press, Cambridge.

Kliman R, Sheehy B, Schultz J (2008) Genetic drift and effective population size. *Nature Education*, **1(3)**, 3.

Knapp AK et al (1999) The Keystone Role of Bison in North American Tallgrass Prairie. *BioScience*, **49**(1), 39-50.

Meagher MM (1973) *The bison of Yellowstone National Park*. National Park Service, Government Printing Office, Washington, D.C.

Nei M, Maruyama T, Chakraborty R (1975) The bottleneck effect and genetic variability in populations. *Evolution*, **29(1)**, 1-10.

Nei M, Roychoudhury AK (1974) Sampling variances of heterozygosity and genetic distance. *Genetics*, **76**, 379-390.

Pinzone CA, Dyer KA (2013) Association of polyandry and sex-ratio drive prevalence in natural populations of *Drosophila neotestacea*. *Proceedings of the Royal Society B*, **280**, 1-8.

Polziehn RO, Strobeck CM, Sheraton J, Beech R (1995) Bovine mtDNA discovered in North American bison populations. *Conservation Biology*, **9**, 1638–1643.

Pritchard JK, Stephens M, Donnelly P (2000) Inference of population structure using multilocus genotype data. *Genetics*, **155**, 945–959.

Putman AI, Carbone I (2014) Challenges in analysis and interpretation of microsatellite data for population genetic studies. *Ecology and Evolution*, **4(22)**, 4399–4428.

Randi E (2008) Detecting hybridization between wild species and their domestic relatives. *Molecular Ecology*, **17**, 285-293.

Robertson A (1955) Selection in animals: synthesis. *Cold Springs Harbor Symposium on Quantitative Biology*, **20**, 225-230.

Rius M, Darling JA (2014) How important is intraspecific genetic admixture to the success of colonizing populations? *Trends in Ecology & Evolution*, **29(4)**, 233–242.

Sanderson EW, Redford KH, Weber B et al. (2008) The ecological future of the North American bison: conceiving long-term, large-scale conservation of wildlife. *Conservation Biology*, **22**, 252–266.

Schnabel RD, Ward TJ, Derr JN (2000) Validation of 15 microsatellites for parentage testing in North American bison, *Bison bison* and domestic cattle. *Animal Genetics*, **31**, 360-366.

Ward TJ, Bielawski JP, Davis SK et al. (1999) Identification of domestic cattle hybrids in wild cattle and bison species: a general approach using mtDNA markers and the parametric bootstrap. *Animal Conservation*, **2**, 51–57.

Wilson GA, Strobeck CM (1999) Genetic variation within and relatedness among wood and plains bison populations. *Genome*, **42**, 483-496.

ALK-EML$_4$-Positive Cancers and Combination Therapy
Probing the Apoptotic Threshold

Teagan H. Glass

The following is an excerpt from a longer piece. For full text, please visit www.honorsjournal.com.

[…]

ABSTRACT

OF ALL THE diseases currently being researched, lung cancer is one of the most pressing due to its worldwide prevalence and high incidence of fatality. More specifically, non-small cell lung cancers (NSCLC) harboring ALK-EML4 gene fusion mutations are of particular interest to researchers due to their widely documented capability of becoming resistant to specialized treatment, such as kinase inhibition. This project was initiated with the aim of using *in vitro* combination drug treatment to more efficaciously inhibit the growth and survival of H3122 cells, an ALK-EML4-positive NSCLC cell line. In this study, H3122 cells were subjected to combined ALK and histone deacetylase (HDAC) inhibition; two ALK inhibitors, crizotinib and AP23116, were combined with paragazole, a class-1 HDAC inhibitor. Both combinations, crizotinib/paragazole and AP23116/paragazole, were found to produce lower EC$_{50}$ values than single-drug treatment. While each drug pair confers synergistic activity, the latter combination was found to be substantially more potent. ALK and HDAC inhibition in combination proves to be an effective means of treating ALK-EML4-positive cells and could be a successful approach to counteracting acquired drug resistance in cancers with ALK rearrangements.

[…]

RESULTS

Single-Drug Treatments

In order to establish a base line for combination treatments, the response of H3122 cells to each of the therapeutic compounds was determined. Averages were taken from four biological replicates of treatments with each drug: crizotinib, AP26113, and paragazole. For crizotinib, the EC$_{50}$ was determined to be 0.97 µM (*Fig. 1A*). This result is concurrent with another group that established an IC$_{50}$ of 1 µM (Katayama et al. 2012). AP26113 exhibited a higher potency, with an IC$_{50}$ of 0.40 µM (*Fig. 1B*). It is apparent when the curves of the two ALK inhibitors are overlaid that crizotinib produced inferior effects (*Fig. 1C*). The dose-response curve of AP23116 demonstrated a steeper

initial slope of the curve and a larger effect at the same concentrations as crizotinib, indicating higher biological activity and maximal efficacy. Paragazole exhibited the least potency, by far, with an EC_{50} of 3.5 μM (*Fig. 1D*). Perhaps the most striking characteristics of paragazole treatment compared to that of treatment with either ALK inhibitor was the relatively miniscule slope and maximal efficacy of the dose-response. While higher concentrations of paragazole would be necessary to achieve a complete sigmoidal dose-response, the data collected represents the relative ineffectiveness of HDACi on its own. Based on the data produced from single-drug treatments, it is evident that both crizotinib and AP23116 on their own achieve powerful maximal efficacies, as well as potencies at reasonable concentrations, in terms of short-term *in vitro* treatment. Paragazole, on the other hand, exhibits

minimal potency and maximal efficacy, even at concentrations much larger than that of either ALK inhibitor. Clearly, it is the kinase activity of the ALK-EML4 fusion protein that predominantly confers survival. Due to the disparity between the effects of individual HDAC and ALK inhibition, it is not obvious that much stronger activity would be achieved in response to treatment with paragazole in combination of each of the two ALK inhibitors.

Combination BRAID Treatments

The focus of BRAID analysis is being able to quantify synergistic activity between two drugs in combination by creating a response surface model. Drug relationships are represented and evaluated by the κ value, where κ<0, κ=0, and κ>0 are indicative of antagonism, additivity, and synergism, respectively.
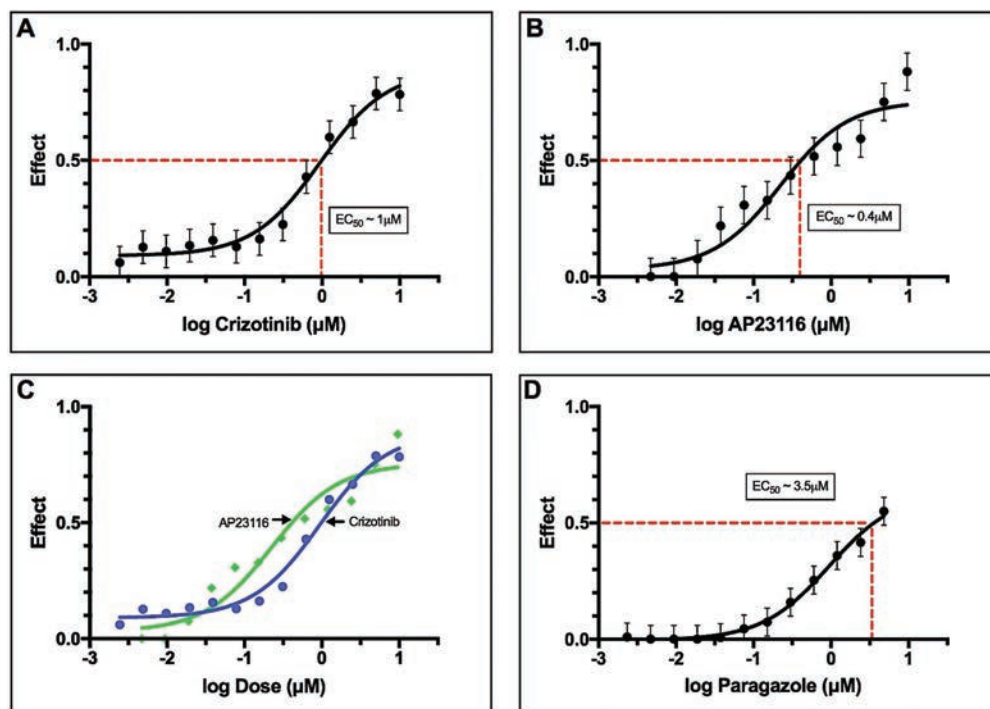

Figure 1. Single-drug dose-responses. (A) Dose-response of H3122 to crizotinib. (B) Dose-response of H3122 to AP21136. (C) Overlay of dose-response of H3122 to crizotinib (blue) & AP23116 (green); arrows indicate location of EC_{50}. (D) Dose-response of H3122 to paragazole.

Drug Combinations	κ Values
AP23116 vs. AP23116	-1.02
Crizotinib vs. crizotinib	-0.42
Paragazole vs. paragazole	0.32

Figure 2. BRAID results for self-self crosses.

A crucial element of the experiment is establishing the baseline activity of each individual drug. This was done by treating H3122 with crizotinib, AP23116, and paragazole "in combination" with themselves in order to achieve purely additive responses. These self-self combinations yielded κ values very close to zero (*Fig. 2*). The slight deviation of these values from κ=0 is not indicative of antagonism, in the case of ALK self-self trial, or synergism, in the case of the HDAC self-self trial, but rather demonstrates that the set-up for the experiment was less than perfect; the numerous intensive and tedious steps of the drug addition process for BRAID analysis yield many opportunities for small errors to be made. The presented data were produced from two biological replicated of each combination.

Establishing an additive baseline with the self-self trials is necessary to accurately determine the relationship between ALK and HDAC inhibitors when H3122s were treated with the two combinations: crizotinib/paragazole and AP23116/paragazole. In order to verify the combination response, each drug pair is tested on two microplates, with the two drugs added in two different orientations. For each combination, crizotinib/paragazole and AP23116/paragazole, κ values of well over zero were produced, indicating strong synergistic activity for each

ALKi/HDACi pair (*Fig. 3*). Not only do the κ values confer synergy, but so do the response surfaces produced by the BRAID analysis (*Fig. 4*). The key feature of a synergistic surface response is the rounding of the response as the concentrations of each drug increase. This is clearly seen in both the crizotinib/paragazole (*Fig. 4A)* and AP23116/paragazole (*Fig. 4B)* response surfaces. This rounding indicates that as the concentration of one drug increases, less and less of the other drug is required to produce the same effect, exemplifying a synergistic relationship between each ALK inhibitor and paragazole. All results yielded positive k values, yet with varying magnitudes due to imperfect drug addictions. While BRAID analysis is indeed a powerful tool, it is difficult to obtain clean results since such a large number of parameters must be addressed. Imperfect drug addiction caused variability in responses for each drug. Synergistic activity was observed in all trials of both ALKi/HDACi combinations, but due to the complicated nature of the set-up, we decided to move towards more straightforward combination treatments that would allow more definitive results to be obtained.

Drug Combinations	κ Values
AP23116 vs. Paragazole (Orientation 1)	100
Paragazole vs. AP23116 (Orientation 2)	100
Crizotinib vs. Paragazole (Orientation 1)	100
Crizotinib vs. Paragazole (Orientation 2)	100

Figure 3. BRAID results for combination crosses.

Simple Combination Treatments

For these combination treatments, results were obtained from four biological replicates of experiments in which H3122 cells were treated with either the crizotinib/paragazole or AP23116/paragazole combination. Cells were treated with combinations ranging from 0.1-9.6 µM in order to achieve complete dose-responses. While both ALK inhibitors and paragazole were sampled in varying ratios to each other, the presented results are of 1:1 ALK/paragazole treatments. When H3122s were treated with crizotinib in combination with paragazole, the observed EC_{50} was 0.7 µM (concentration of each drug) (*Fig. 5A*). In terms of synergy, the combination is not drastically more effective than crizotinib on its own (EC_{50} 0.97 µM). However, when compared to crizotinib by itself, crizotinib and paragazole in combination do exhibit a higher potency and biological activity (steeper slope), as well as higher maximal efficacy (*Fig. 5C*).

The combination of AP23116 and paragazole, on the other hand, exhibited marked effectiveness, with an EC_{50} of 0.04 µM (*Fig. 5B*). When overlaid with single-drug AP23116 treatment, the dose-response of combination treatment is indicative of substantially higher biological activity and potency (Fig. 5D). The EC_{50} of the combination is more than ten-fold less than that of AP23116 alone (0.04 µM vs. 0.6 µM, respectively). Clearly, H3122 cells are vastly more sensitive to the combined action of AP23116 and paragazole than any single-drug treatment. Something to note is the irregular shape of the dose-response curve of the AP23116/paragazole combination; while all other treatments can be closely fit
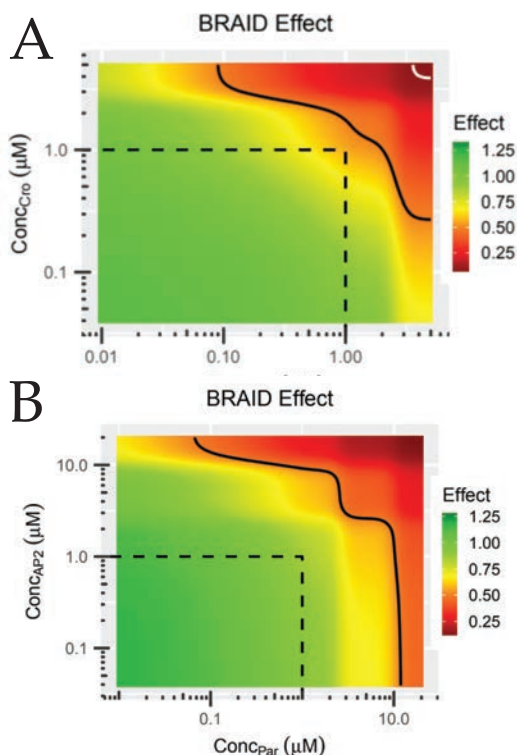

Figure 4. BRAID response surfaces for combination trials. HDACi concentration is plotted on the x-axis; ALKi concentration is plotted on the y-axis. (A) Crizotinib vs. paragazole. (B) AP23116 vs. paragazole.

with normal sigmoidal response curves, this combination exhibits a parabolic dose-response (*Fig. 5B*). Among all four biological replicates, there were no significant outliers or irregularities, leading me to believe that this dose-response is valid. This shape is indeed irregular, but the steepness of the curve is due to substantial effects at very low concentrations of AP23116 and paragazole, emphasizing the efficacy of the combination. AP23116 exhibits an EC_{50} of more than two-fold less than crizotinib, yet when combined with paragazole, the AP23116 produces a much larger-fold increase in efficacy. Evidently, potent ALK inhibition sensitizes H3122s to HDAC inhibition to a greater extent.
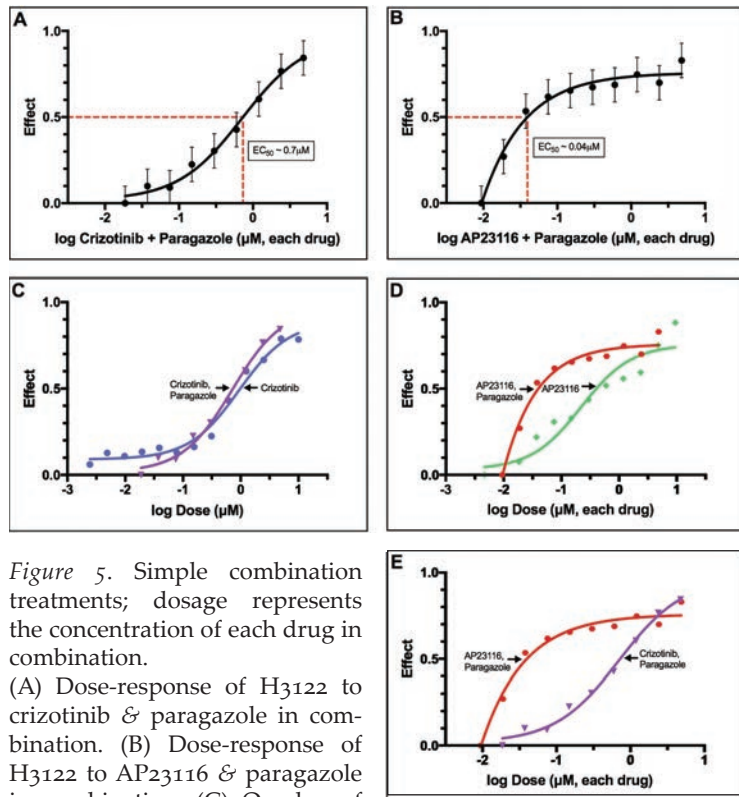
48

Figure 5. Simple combination treatments; dosage represents the concentration of each drug in combination.
(A) Dose-response of H3122 to crizotinib & paragazole in combination. (B) Dose-response of H3122 to AP23116 & paragazole in combination. (C) Overlay of dose-responses of H3122 to crizotinib (blue) and crizotinib & paragazole in combination (purple); arrows indicate EC$_{50}$ concentration. (D) Overlay of dose-responses of H3122 to AP23116 (green) and AP23116 & paragazole in combination (red); arrows indicate EC$_{50}$ concentration. (E) Overlay of dose-responses of H3122 to crizotinib & paragazole in combination (purple) and AP23116 & paragazole in combination (red); arrows indicate EC$_{50}$ concentration.

Staggered Combination Treatments

Since synergistic activity was observed with each ALKi/HDACi combination, staggered combination experiments were conducted in order to establish if the observed effects were dependent on ALKi or HDACi. These experiments were done by initially treating H3122s with one drug, followed by the addition of the other drug of the pair after 24 hours. Both combinations yielded stronger responses when ALKi was the initial treatment. As expected, due to the difference in potency between the two ALK inhibitors, the initial addition of AP23116 exhibited higher potency and biological activity (*Fig.*

6B) compared to when crizotinib was the initial treatment (*Fig. 6A*). Also, as expected, a higher potency was achieved when AP23116 was the secondary treatment compared to crizotinib. Due to the fact that survival of ALK+ cancers is highly dependent on constitutive ALK activation, it is not surprising that ALK inhibition appears to be the dominating factor. However, the discrepancy between responses of ALKi as initial vs. secondary treatment could be due to the large difference in potency between both ALK inhibitors and paragazole. Judging by the relatively low efficacy of paragazole single-drug treatment, it would not be expected that HDAC inhibition would lend itself to greater ALKi effectiveness, yet simultaneous combination treatment yields dramatic results. In order to truly determine whether or not the observed synergistic activity is HDAC- or ALK-dependent, comprehensive mechanistic studies would be have to be conducted.

DISCUSSION

Combination therapy is becoming a widely used strategy to more efficaciously treat patients diagnosed with cancers harboring genetic aberration, specifically those which confer drug resistance. Approximately 70,000 people are diagnosed with ALK-EML4-positive non-small cell lung cancer each year (Sasaki et al. 2010). The prevalence of these diagnoses necessitates the formulation of effective, specialized treatments that can overcome the resistance mechanisms of the ALK-EML4 gene fusion. While tyrosine kinase inhibitors (TKI) continue to be used in clinical trials to treat these patients to inhibit the kinase activity of the fusion
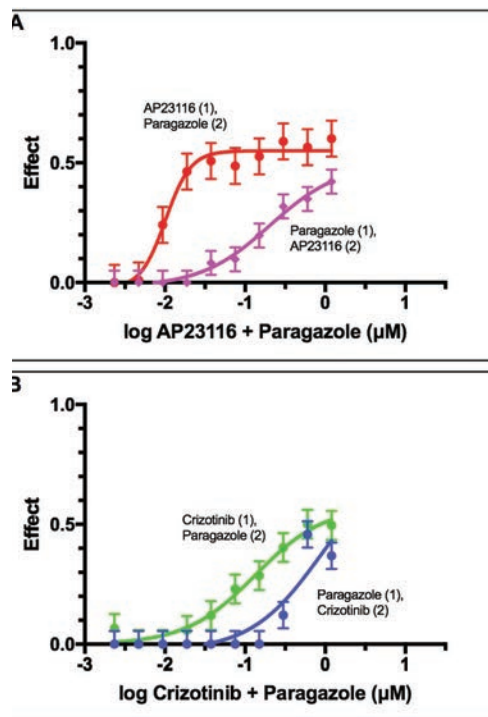
Figure 6. Staggered combination treatments; dosage represents the concentration of each drug in combination. (1) denotes initial treatment, while (2) denotes secondary treatment after 24 hours. (A) Overlay of dose-responses of crizotinib & paragazole in combination. (B) Overlay of dose-responses of AP23116 & paragazole in combination.

product, acquired drug resistance to ALK inhibition therapy is nearly inevitable. Therapeutic combinations are a promising method to overcome resistance mechanisms such as ALK gene amplification and point mutations in the ALK kinase domain. In this project, it was found that combining of ALK inhibitors (crizotinib or AP23116) with the HDAC inhibitor, paragazole, produces synergistic effects that are considerably more effective than any of the three single-drug treatments. While the AP23116/paragazole combination was found to be more potent than crizotinib/paragazole, this confirms that combined ALK and HDAC inhibition is a valid potential therapeutic approach to treating ALK-EML4 can-

cers. Definitively inducing cell death in ALK-EML4 tumors would prevent acquired drug resistance from occurring in wild-type cells and inhibit survival of those with resistance-related mutations.

From a mechanistic perspective, there are numerous studies that rationalize the synergistic effects of combined ALK and HDAC inhibition. Many selective TKIs have been found to effectively induce apoptosis in ALK-EML4 NSCLC. ALK inhibition induces expression of key pro-apoptotic factors and represses pro-survival factors by markedly abrogating phosphorylation of ALK, ERK, and STAT3 (Katayama et al. 2012; Takezawa et al. 2011). ALK inhibitors such as crizotinib and AP23116, among many others, have known therapeutic value, and understandably so since ALK-EML4 cells rely on constitutive ALK activation for survival and proliferation. So why does class-I HDAC inhibition, a less powerful treatment, yield ALK-EML4 lung cancer that much more sensitive to ALKi therapy? The key may be that these cancers greatly rely upon HDAC activity on both histone and non-histone substrates to survive, in addition to ALK activation. HDAC expression has been implicated with mediating tumor progression in a variety of cancers (Damaskos et al. 2018). Furthermore, a variety of HDAC inhibitors, including quisinostat and trichostatin A (TSA), have been found to induce both intrinsic and extrinsic apoptotic pathways in various lung cancers (Miyanaga et al. 2008). It has been reported that HDACi activates extrinsic death receptor pathways, such as tumor necrosis factor (TNF), by up-regulating various TNF receptors as well as their ligands at the transcriptional level

(Zhang et al. 2014). HDACi has also been shown to induce intrinsic apoptotic pathways via p53 activation. By inactivating nuclear histone deacetylases, p53 becomes hyperacetylated, preventing its inactivation via ubiquitination by MDM2 (Zhuang 2013). p53 activation induces expression of many downstream pro-apoptotic factors of the Bcl-2 family, such as Bim. Zhang et al. reports that transcriptional activation of pro-apoptotic Bcl-2 factors is also mediated by hyperacetylation of the H3 and H4 histone subunits, a result of class-I HDAC inhibition. Bao et al. also observed this hyperacetylation of H3 and H4 as a result of quisinostat treatment. Finally, HDAC inhibition has been shown to abrogate STAT3 activity, an essential transcriptional regulator of factors that promote cell survival, growth, proliferation, and differentiation (Takezawa et al. 2011). Hyperacetylation of STAT3 due to HDACi has been shown to inhibit its phosphorylation and catalyze its translocation from the nucleus to the cytoplasm, therefore diminishing its capability to induce transcription of its downstream factors (Gupta et al. 2009; Zhuang 2013).
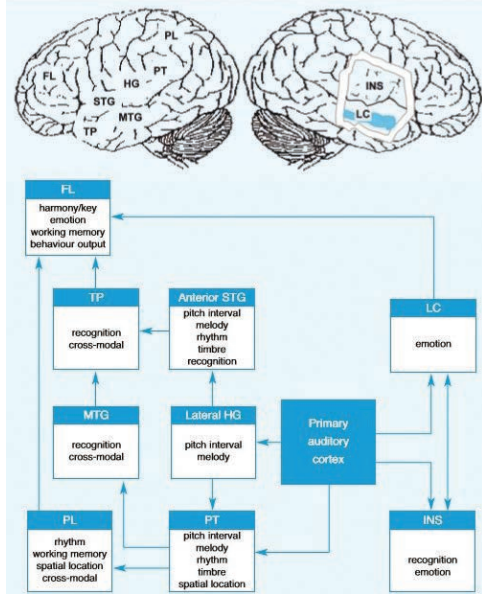
The fact that both ALKi and HDACi produce overlapping and non-overlapping effects in terms of stimulating pro-apoptotic pathways could very well explain the synergistic relationship between the two inhibitors when administered to ALK-EML4 cancers. When combined with depletion of ALK and STAT3 activity via ALKi, concurrent activation of the TNF pathway, along with the up-regulation of pro-apoptotic Bcl-2 proteins via p53 induction and histone hyperacetylation, HDACi may overcome pro-survival mechanisms utilized by ALK-EML4 NSCLCs. Certainly a threshold is reached wherein the pro-apoptotic effects of ALK and HDAC inhibition overcome all pro-survival pathways and induce cell death. While much mechanistic-focused work must be done to validate this hypothesis, recent research, as well as the data presented in this paper, confirms the legitimacy of combining ALKi with HDACi as a means of treating ALK-EML4 cancers. In addition to establishing the precise mechanisms that confer synergy between these two drugs, employing this combination therapy on ALK-EML4 cells that exhibit ALKi-resistance would further the validity and value of this particular approach. Only by formulating a specialized treatment that is capable of overcoming acquired drug resistance to ALKi therapy can we improve the quality and longevity of life of those diagnosed with ALK-EML4-positive cancers.

Works Cited

Bao, Lianmin, Hua Diao, Nian Dong, Xiaoqiong Su, Bingbin Wang, Qiongya Mo, Heguo Yu, Xiangdong Wang, and Chengshui Chen. "Histone Deacetylase Inhibitor Induces Cell Apoptosis and Cycle Arrest in Lung Cancer Cells via Mitochondrial Injury and P53 Up-Acetylation." *Cell Biology and Toxicology* 32, no. 6 (December 1, 2016): 469–82.

Bayliss, Richard, Jene Choi, Dean A. Fennell, Andrew M. Fry, and Mark W. Richards. "Molecular Mechanisms That Underpin EML4-ALK Driven Cancers and Their Response to Targeted Drugs." *Cellular and Molecular Life Sciences* 73 (2016): 1209–24.

Chia, Puey Ling, Paul Mitchell, Alexander Dobrovic, and Thomas John. "Prevalence and Natural History of ALK Positive Non-Small-Cell Lung Cancer and the Clinical Impact of Targeted Therapy with ALK Inhibitors." *Clinical Epidemiology* 6 (November 20, 2014): 423–32.

Chiarle, Roberto, Claudia Voena, Chiara Ambrogio, Roberto Piva, and Giorgio Inghirami. "The Anaplastic Lymphoma Kinase in the Pathogenesis of Cancer." *Nature Reviews Cancer* 8, no. 1 (January 2008): 11–23.

Damaskos, Christos, Ioannis Tomos, Nikolaos Garmpis, Anna Karakatsani, Dimitrios Dimitroulis, Anna Garmpi, Eleftherios Spartalis, et al. "Histone Deacetylase Inhibitors as a Novel Targeted Therapy Against Non-Small Cell Lung Cancer: Where Are We Now and What Should We Expect?" *Anticancer Research* 38, no. 1 (January 1, 2018): 37–43.

Gupta, Mamta, Mary Stenson, Terra Lasho, Ayalew Tefferi, Anne Novak, Stephen M. Ansell, and Thomas E. Witzig. "Interplay Between Histone Deacetylases (HDACs) and STAT3: Mechanism of Activated JAK/STAT3 Oncogenic Pathway in ABC (Activated B-Cell) Type Diffuse Large B Cell Lymphoma." *Blood* 114, no. 22 (November 20, 2009): 925–925.

Heuckmann, Johannes M., Hyatt Balke-Want, Florian Malchers, Martin Peifer, Martin L. Sos, Mirjam Koker, Lydia Meder, et al. "Differential Protein Stability and ALK Inhibitor Sensitivity of EML4-ALK Fusion Variants." *Clinical Cancer Research* 18, no. 17 (September 1, 2012): 4682–90.

Katayama, Ryohei, Tahsin M. Khan, Cyril Benes, Eugene Lifshits, Hiromichi Ebi, Victor M. Rivera, William C. Shakespeare, A. John Iafrate, Jeffrey A. Engelman, and Alice T. Shaw. "Therapeutic Strategies to Overcome Crizotinib Resistance in Non-Small Cell Lung Cancers Harboring the Fusion Oncogene EML4-ALK." *Proceedings of the National Academy of Sciences of the United States of America* 108, no. 18 (May 3, 2011): 7535–40.

Katayama, Ryohei, Alice T. Shaw, Tahsin M. Khan, Mari Mino-Kenudson, Benjamin J. Solomon, Balazs Halmos, Nicholas A. Jessop, et al. "Mechanisms of Acquired Crizotinib Resistance in ALK-Rearranged Lung Cancers." *Science Translational Medicine* 4, no. 120 (February 8, 2012): 120ra17-120ra17.

Li, Yongjun, Xiaofen Ye, Jinfeng Liu, Jiping Zha, and Lin Pei. "Evaluation of EML4-ALK Fusion

Lobe	Canonical Distribution	Percentage
Left frontal	23.74%	27.66%
Right frontal	24.02%	28.37%
Left Parietal	11.17%	7.09%
Right Parietal	5.87%	4.96%
Left temporal	3.91%	1.42%
Right temporal	6.98%	3.55%
Left occipital	11.73%	12.06%
Right occipital	12.57%	14.89%

Table 1. Distribution of brain activity due to music stimuli. Fang et al. (2015).

Fang et al. (2015) also correlated music to language and found that both music and speech involve perception, action, learning, memory, and emotion. They led a data-driven analysis in which participants underwent a natural stimulus functional MRI (N-fMRI) while music and speech were used as stimuli. It was found that music and speech produced almost the same results, with distribution of activity as shown in Table 1 (Fang et al., 2015).

[…]

While fMRI proves to be a consistent and reliable tool for studying the brain, electroencephalogram (EEG) is another way to determine the exact locations of the brain that processes music (Nizamie and Tikka, 2014). It was discovered that the acoustic circuit involves the auditory nerve, brainstem, medial geniculate, body of the thalamus, and auditory cortex (Nizamie and Tikka, 2014). Not only do these areas of the brain strongly correlate to the limbic system, but after undergoing music ther-

apy, schizophrenia patients showed significant changes in the frontal EEG after undergoing music therapy sessions (Nizamie and Tikka, 2014), which is strong evidence that music does in fact have a noteworthy effect on the brains of both healthy and unhealthy individuals.

Certainly, if music can affect the brain in many different areas, there must be additional processes that are affected as well. In fact, music involves cortical systems extending well beyond auditory cortices and affects not only heart rate and respiratory rate, but capnography as well (Stewart et al., 2006). Capnography is the measure of carbon dioxide output and can often relate to the mental state of a patient, such as sleepiness, alertness, and calmness. This connection may lead to the ability to monitor carbon dioxide output along with music stimuli to diagnose certain psychiatric conditions, making the diagnosis more accurate and affordable than the conventional methods.

PSYCHIATRIC DISORDERS AND THE BRAIN

While there is very little research connecting the effects of music on specific psychiatric disorders,

there is a fair amount of documented functional imaging of disorders and the areas of the brain they effect. In order to ensure that music would affect the brain during an fMRI, Stewart et al. (2006) found that certain musical listening disorders did in fact show significant differences in activation with music stimuli. Stewart et al. (2006) also found that Alzheimer's produced increased perfusion in the left temporal lobe and angular gyrus, and that musical hallucinations often occurred in patients with depression, schizophrenia, obsessive-compulsive disorder, and alcoholism. This review will not focus on Alzheimer's or alcoholism, but the research done by Stewart is worth mentioning as it is one of the only studies connecting music and psychiatric disorders during functional imaging.

Personality disorders are a common issue in today's society but is frequently misdiagnosed, with only approximately 71.7% of diagnoses remaining constant upon a second evaluation by a psychiatrist (Merten et al., 2017). There are many types of personality disorders, but the most common are bipolar disorder, antisocial personality disorder, and narcissistic personality disorder. Bipolar disorder (BD) happens to be the most common of the three, and upon using manual tracing methods with fMRI, BD shows affective and behavioral dysregulation, impairments of prosody and interpersonal connections, and disturbed relatedness, as well as smaller grey matter volume in the amygdala and hippocampus (Schulze and Roepke, 2014; Frangou et al.,

2014). These findings are significant in relation to this review because the amygdala and hippocampus are both involved in processing music, and the impairments in prosody shown could relate to how a person with BD would react to music. Antisocial personality disorder (APD) and narcissistic personality disorder (NPD) both showed lower activation of the amygdala with orbitofrontal and ventromedial implications (Shulze and Roepke, 2014). The subtle differences between BD and NPD is key in looking for potential diagnostic abilities, as BD focuses on a smaller grey matter of the amygdala, while NPD focuses on lower activation, as shown by Figure 2.
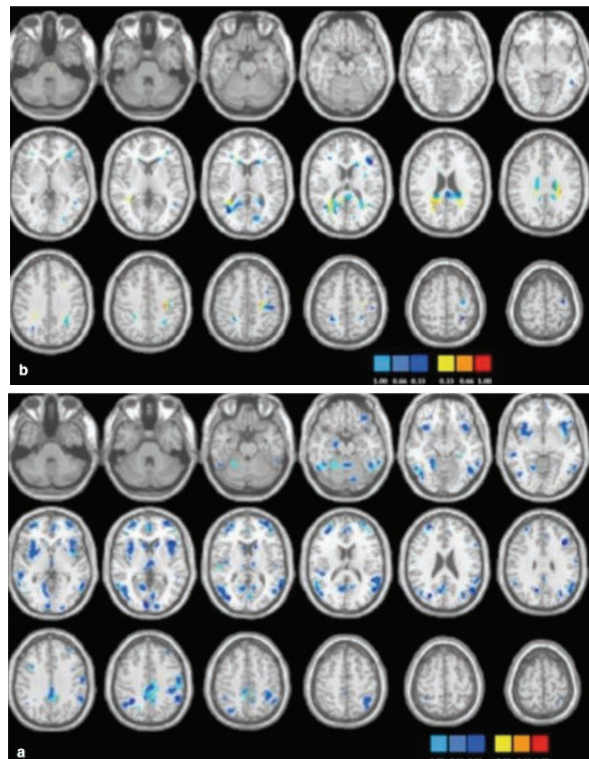
[…]

Figure 2. Discrimination maps for grey matter (a) and white matter (b) classification between patients with bipolar disorder and healthy individuals. Frangou et al. (2014)

Major depression disorder (MDD) is another common psychiatric disorder, though it is frequently misdiagnosed and research suggests that antidepressants are a less effective treatment than music therapy (Nizamie and Tikka, 2014). The subgenual cingulate, thalamus, and orbitofrontal cortex were all activated at a much higher rate than healthy individuals (Greicius et al., 2007). In addition, the entorhinal cortex (EC) showed extreme asymmetry between the orbital and medial prefrontal cortex (OMPFC) and the amygdala when subjects were asked to classify happy faces during fMRIs, specifically involving left-sided differences involving top-down connections (Almeida et al., 2009). One of the most unique features of major depression in functional imaging is the asymmetry in the EC, but it should be noted that Almeida et al. (2009) were only able to replicate the results with female participants and while providing the specific stimulus of classifying happy faces. As common as MDD is, there is little research on the functional imaging of MDD, especially using music or language as a stimulus. The most consistent unique feature seems to be increased activation of the thalamus and orbitofrontal cortex, as illustrated by Figure 3 (Greicius et al., 2007).

Schizophrenia is often considered one of the most extreme psychiatric disorders, as it produces symptoms that severely interfere with the lives of patients and there is no cure. Upon analyzing fMRIs of patients with schizophrenia stimulated by a word monitoring task, Tagaments et al. (2014) found that the cuneus, lingual gyrus, medial superior frontal gyrus, bilateral middle superior/ middle temporal gyrus, posterior visual areas, medial superior frontal
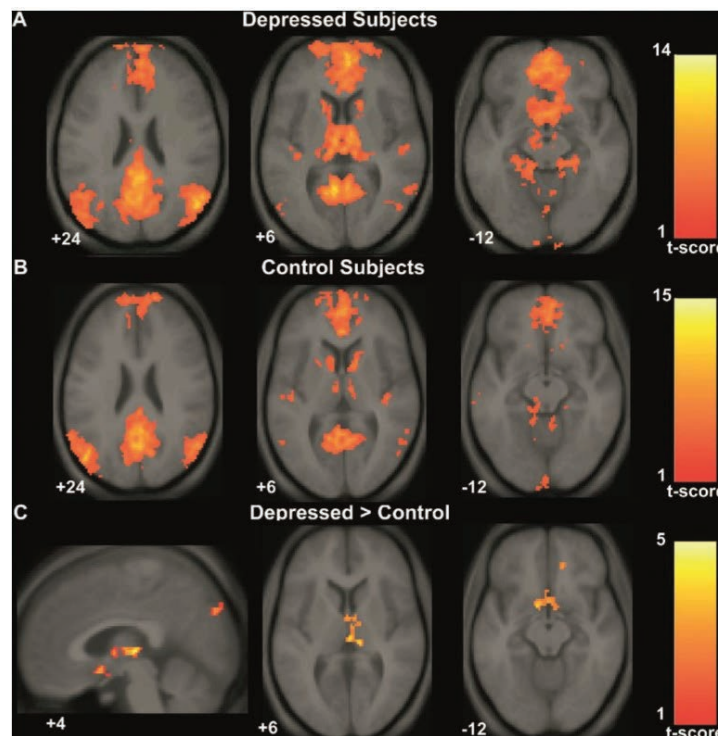

Figure 3. Functional MRI differences between healthy and depressed individuals. Greicius et al. (2007)

gyrus, left middle/superior frontal cortex, and right precentral cortex all showed differences when compared to healthy individuals. Schizophrenia is the most complicated with regards to the number of regions activated, but can be easily identifiable when compared to other psychiatric disorders' fMRIs as one would see incredible differences in nearly all regions of the brain. Though Tagaments et al.'s (2014) research was speech based, my hypothesis is that using music as stimuli would produce similar results, as many have concluded that music is a form of communication (Stewart et al., 2006; Fang et al., 2015; Warren, 2008). Schizophrenia is not well studied at this point and requires much more research in order to include it in disorders that music would be able to diagnose.

CONCLUSION

In summary, all psychiatric disorders discussed present with differences in the amygdala, insula, orbitofrontal regions, lingual gyrus, or cingulate gyrus, which are all regions connected to the processing of music in healthy individuals as well. There are unique differences for each disorder which lends to the hypothesis that music may be a reliable stimulus that produces unique results when studying functional imaging of the brain. While there is a significant amount of research that has been done studying music and the brain in healthy individuals and functional imaging of some psychiatric disorders, research in the field of music psychophysiology is hardly complete. There is enough information to build a foundation for future research, but more research is needed to create consistent findings in the functional imaging of some disorders, such as in schizophrenia, depression, and others not mentioned in this review.

[…]

Based on the information given by the current research, it can be concluded that psychiatric disorders would show differences in the brain when stimulated with music and it may be hypothesized that one could use music in conjunction with fMRI to diagnose the aforementioned psychiatric disorders. If researchers are able to find a correlation between vitals, music, and specific disorders while listening to music that is both unique to the disorder and reliable, affordable healthcare, diagnosis, and treatment of psychiatric disorders may be brought to the community and change the means, accuracy, and costs of mental health issue diagnosis and treatment.

Works Cited

60

Almeida, J. R. C. de, Versace, A., Mechelli, A., Hassel, S., Quevedo, K., Kupfer, D. J., & Phillips, M. L. (2009). Abnormal Amygdala-Prefrontal Effective Connectivity to Happy Faces Differentiates Bipolar from Major Depression. *Biological Psychiatry*, *66*(5), 451–459.

Erkkilä, J., Gold, C., Fachner, J., Ala-Ruona, E., Punkanen, M., & Vanhala, M. (2008). The Effect of Improvisational Music Therapy on the Treatment of Depression: Protocol for a Randomised Controlled Trial. *BMC Psychiatry*, *8*, 50.

Fang, J., Hu, X., Han, J., Jiang, X., Zhu, D., Guo, L., & Liu, T. (2015). Data-Driven Analysis of Functional Brain Interactions During Free Listening to Music and Speech. *Brain Imaging and Behavior*, *9*(2), 162–177.

Frangou, S. (2014). The Structural and Functional Neuroanatomy of Bipolar Disorder. In *MRI in Psychiatry* (pp. 303–311). Springer, Berlin, Heidelberg.

Gavrielidou, M., & Odell-Miller, H. (2017). An Investigation of Pivotal Moments in Music Therapy in Adult Mental Health. *The Arts in Psychotherapy*, *52*(Supplement C), 50–62.

Gawrysiak, M. J., Carvalho, J. P., Rogers, B. P., Nicholas, C. R. N., Dougherty, J. H., & Hopko, D. R. (2012). Neural Changes following Behavioral Activation for a Depressed Breast Cancer Patient: A Functional MRI Case Study. *Case Reports in Psychiatry; New York*. Retrieved from Gawrysiak, M. J., Swan, S. A., Nicholas, C. R. N., Rogers, B. P., Dougherty,

J. H., & Hopko, D. R. (2013). Pragmatic Psychodynamic Psychotherapy for a Patient with Depression and Breast Cancer: Functional MRI Evaluation of Treatment Effects. *American Journal of Psychotherapy; New York*, *67*(3), 237–55.

Greicius, M. D., Flores, B. H., Menon, V., Glover, G. H., Solvason, H. B., Kenna, H., … Schatzberg, A. F. (2007). Resting-State Functional Connectivity in Major Depression: Abnormally Increased Contributions from Subgenual Cingulate Cortex and Thalamus. *Biological Psychiatry*, *62*(5), 429–437.

Immordino-Yang, M. H., & Singh, V. (2013). Hippocampal Contributions to the Processing of Social Emotions. *Human Brain Mapping*, *34*(4), 945–955.

Krumhansl, C. L. (1997). An Exploratory Study of Musical Emotions and Psychophysiology. *Canadian Journal of Experimental Psychology; Old Chelsea, Quebec*, *51*(4), 336–353.

Kurysheva, I. (2008). Fundamental Psychophysiology of Music Therapy of Neurological Diseases. *International Journal of Psychophysiology*, *69*(3), 302.

Merten, E. C., Cwik, J. C., Margraf, J., & Schneider, S. (2017). Overdiagnosis of Mental Disorders in Children and Adolescents (in Developed Countries). *Child and Adolescent Psychiatry and Mental Health*, *11*, 5.

Mula, M., & Trimble, M. R. (2009). Music and Madness: Neuropsychiatric Aspects of Music. *Clinical Medicine*, *9*(1), 83–86.

Nizamie, S. H., & Tikka, S. K. (2014). Psychiatry and Music. *Indian Journal of Psychiatry*, *56*(2),

128–140.

Rogalsky, C., Rong, F., Saberi, K., & Hickok, G. (2011). Functional Anatomy of Language and Music Perception: Temporal and Structural Factors Investigated Using fMRI. *The Journal of Neuroscience : The Official Journal of the Society for Neuroscience, 31*(10), 3843–3852.

Schulze, L., & Roepke, S. (2014). Structural and Functional Brain Imaging in Borderline, Antisocial, and Narcissistic Personality Disorder. In *MRI in Psychiatry* (pp. 313–340). Springer, Berlin, Heidelberg.

Smith, R., Fadok, R. A., Purcell, M., Liu, S., Stonnington, C., Spetzler, R. F., & Baxter, L. C. (2011). Localizing Sadness Activation Within the Subgenual Cingulate in Individuals: a Novel Functional MRI Paradigm for Detecting Individual Differences in the Neural Circuitry Underlying Depression. *Brain Imaging and Behavior; Indianapolis, 5*(3), 229–39.

Spoormaker, V. I., Vermetten, E., Czisch, M., & Wilhelm, F. H. (2014). Functional Neuroimaging of Anxiety Disorders. In *MRI in Psychiatry* (pp. 289–301). Springer, Berlin, Heidelberg.

Stanard, R. P. (2000). Assessment and Treatment of Adolescent Depression and Suicidality. *Journal of Mental Health Counseling; Alexandria, 22*(3), 204–217.

Stewart, L., von Kriegstein, K., Warren, J. D., & Griffiths, T. D. (2006). Music and the Brain: Disorders of Musical Listening. *Brain, 129*(10), 2533–2553.

Tagamets, M. A., Cortes, C. R., Griego, J. A., & Elvevåg, B. (2014). Neural Correlates of the Relationship Between Discourse Coherence and Sensory Monitoring in Schizophrenia. *Cortex, 55,* 77–87.

Warren, J. (2008). How Does the Brain Process Music? *Clinical Medicine, 8*(1), 32–36.